STUDY OF THE MIXED FLOWS TURBOFAN THRUST FOCUSED ON THERMODYNAMIC PARAMETERS AND ENGINE OPERATING REGIMES

Irina-Carmen ANDREI
INCAS National Institute for Aerospace Research "Elie Carafoli", andrei.irina@incas.ro

Gabriela STROE
POLITEHNICA University of Bucharest, Faculty of Aerospace Engineering, ing.Stroe@yahoo.com, ORCID: 0000-0003-1275-4590

Mihaela-Luminița COSTEA
INCAS National Institute for Aerospace Research "Elie Carafoli", icandrei28178@gmail.com

DOI: 10.19062/1842-9238.2020.18.1.4

Abstract: *The study presented in this paper is focused on highlighting how the thrust as the main performance of the mixed flows turbofan engine is influenced by the airspeed, flight altitude and engine operation speed regime variation. Based on the performances (thrust, specific thrust and fuel specific consumption) of the mixed flow turbofan engine, the Engine Maps (Altitude Map, Velocity Map and Speed Map) can be expressed. The mathematical model describing the operation of the mixed flows turbofan engine is based on the assumptions of fixed geometry engine, fluid flow consisting of perfect gas, with the consideration of different species (i.e. air as cold stream, fuel and a mixture of burned gas as hot stream), Brayton cycle described by isentropic, adiabatic thermodynamic evolutions, including losses that generate an increase in entropy. For further developments, the mathematical model of the engine can be expanded with the variable geometry hypothesis. From the numerical simulations based on the mathematical model of the mixed flows turbofan engine, the correlations of thrust with flight Mach number and engine operation speed regime conclude the study that describes the behavior of the engine from the standpoint of thermodynamics, flight and engine operating regimes.*

Keywords: *mixed flows turbofan engine, performances, thrust, flight regimes, engine operating regimes, Mach number, mathematical modeling, numerical simulations.*

1. INTRODUCTION

The turbofan engines are widely used in civil and military aircraft. With respect to the turbojet engines, the turbofan engines prove significant advantages that contribute to increased safety in operation, Cumpsty [1], Fowler [2], Mattingly [3-4], Farokhi [5].

For the entire flight envelope, the turbofan engines, due to the multiple spool architecture, the operating line of the engine is shifted at a significant safer distance from the surge line, by the means of the advanced engine control systems [9-12], [22-24].

The most used multiple spool solutions are twin -spool and then triple-spool. For more than four spools, the designed construction of the engine supposes higher costs due to the enlargement of the cross section and significant increase of the global weight, and it also requires intricate engine control systems.

The turbofan engines, which are also referred as high bypass ratio or large bypass ratio are widely used for commercial flights, for civil and military aircrafts. The reasons are the improved fuel economy (in cruise) and noise reduction, [13-14].

2. DESIGN OF ACTUAL TURBOFAN ENGINES

The design of actual turbofan engines includes optimizations on the overall engine efficiency, mitigation of noise and emissions levels [5-8].

The most relevant aspects of engine design and construction are summarized as follows:

Figure 1 illustrates the construction of a modern twin spool turbofan, highlighting its main parts. The core flow passes through the fan (which acts as a Low Pressure Compressor), High Pressure Compressor, Combustion Chamber, High Pressure Turbine, Low Pressure Turbine and Core Nozzle. The Bypass Flow crosses the fan and the Bypass Nozzle. The use of the reverse-flow combustion chamber, as shown in Fig. 1, enables a significant reduction of the engine's weight, by shortening its length.

For military applications there are used the high-bypass turbofans, which are also known as mixed flows turbofan engines.

The reasons are consequences of different priority setting for the military applications focused on combat aircraft, such as:

1. The thrust requirements change rapidly during combat and the response of the low-bypass turbofans to throttle adjustments is faster compared to the high-bypass turbofans; the inertia is less and less air mass is involved (for increasing the velocity).

2. The low-bypass turbofans have less frontal area, thus reducing the drag produced. For aircraft expected to fly at supersonic speeds, however briefly, this is important.

3. Better thrust to weight ratio, e.g. 9:1 for F119 low-bypass ratio (used in F-22 Raptor) versus 6:1 for Trent 1000 high-bypass ratio. Even if the actual thrust produced by the low-bypass turbofans is lesser, they produce more thrust per kg of engine, which means that the engine can be more compact in size.

4. The low-bypass turbofans are more efficient at higher speeds compared to the high-bypass turbofans.

5. The reduced cross section size of the low-bypass turbofans mean that the aircraft can be made stealthier by embedding the engines inside the fuselage, which in case of high-bypass turbofans cannot be achieved.

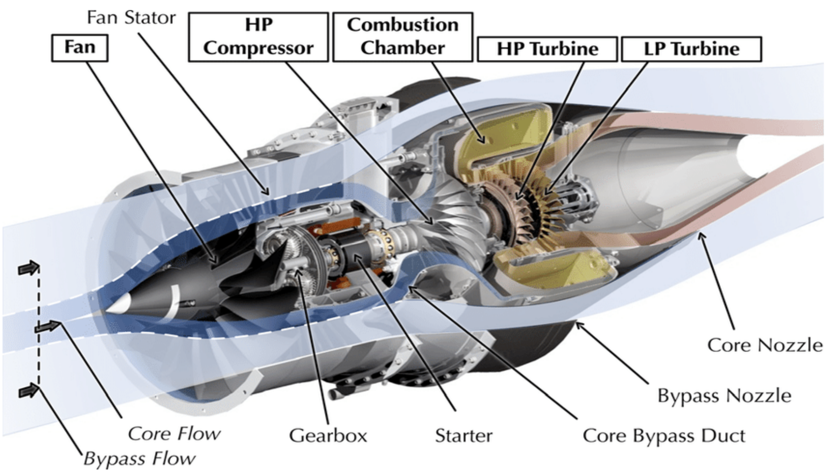

FIG. 1 – Turbofan Engine Parts [6-8]

Figure 2 presents a multiple-spool turbofan construction, with the visualization of the fluid flow path and streamline. For such type of engines, the axial component of the velocity (in core flow as well as in bypass flow) is significantly higher than the radial and tangent components of the velocity, thus resulting lower turbulence levels and consequently reduced noise levels, which demonstrates the environmental friendly feature.

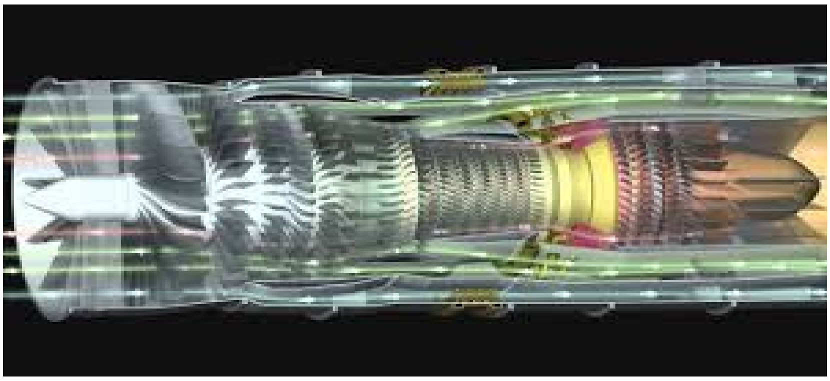

FIG. 2 – Multiple-Spool Turbofan Engine – View of Fluid Flow Path, Streamlines [6-8]

From Fig. 1 and Fig. 2 one can remark that the construction of the combustion chamber determines the axial length of the engine; the direct-flow construction (as indicated in Fig. 2) produces an increase of the engine's axial length, while the reverse-flow construction (as shown in Fig. 1) enables a reduction of the axial length.

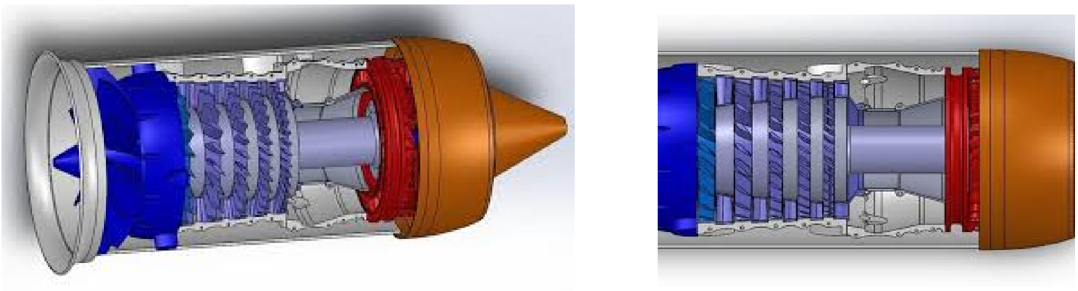

Low- and High-Pressure Compressor-Turbine Group: (left) 3D cut view; (right) cut view

FIG. 3 – Twin-Spool Mixed Flows Turbofan Engine – Schematic Diagrams [6-8]

In Fig. 3 the Low- and High-Pressure Compressor-Turbine Group for a twin-spool construction of Mixed Flows Turbofan Engine are high-lighted.

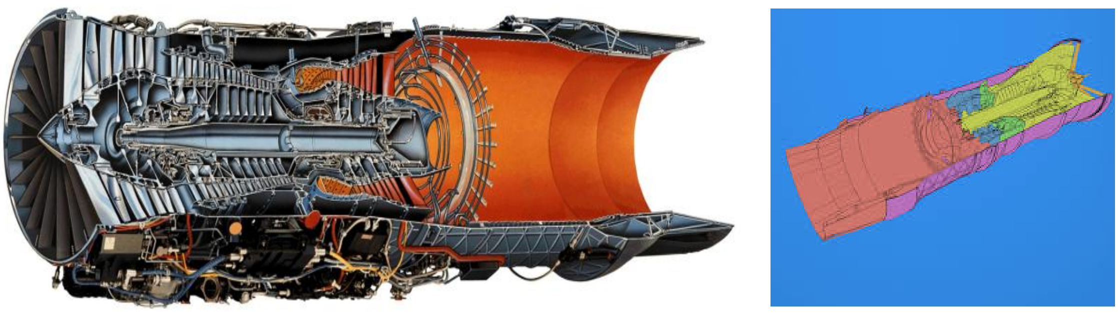

(a) F100 PW 220 Reheated Mixed Flows Turbofan Engine (b) Schematic Diagram

FIG. 4 – Reheated Mixed Flows Turbofan Engine [6-8]

The use of the reheat is a powerful means aimed to augment the thrust of the turbojet and turbofan engines. Referring to the F16 Fighting Falcon, which is currently serving the Romanian Air Force, the propulsion system is the F100 PW 220 Reheated Mixed Flows Turbofan Engine, as shown in Fig. 4.a.

For the supersonic propulsion of the aircraft, mixed flows turbofan engines can be successfully used. For achieving such purpose, the geometry of the aircraft must be adjusted; the main modifications refer to the supersonic inlet and the variable geometry exit nozzle, for both dedicated engine control systems being required.

Figure 5 presents the architectures of supersonic Mixed Flows Turbofan Engine MFTE, designed and manufactured by Rolls Royce and SNECMA.

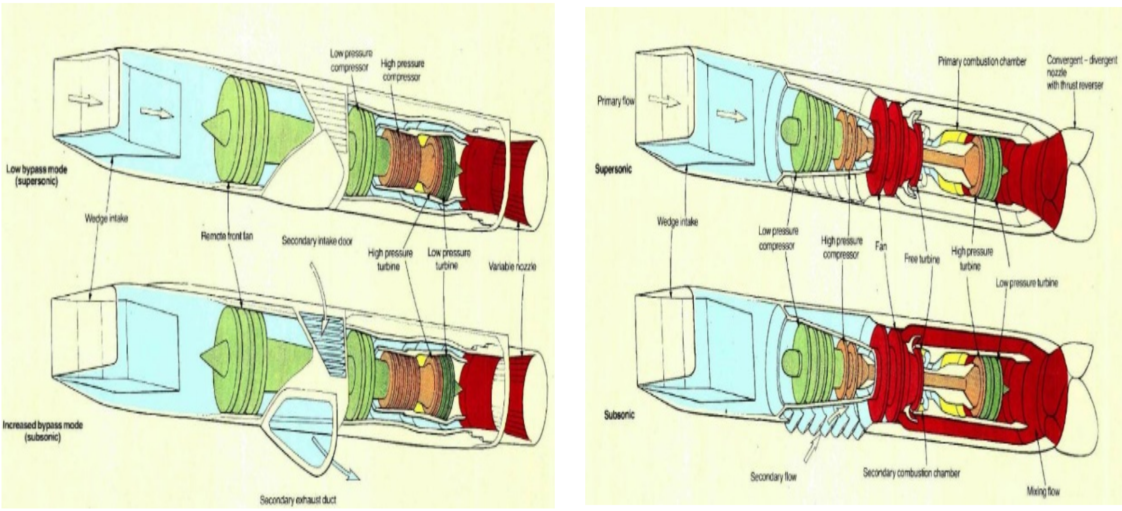

(a) Rolls Royce Architecture (b) SNECMA Architecture

FIG. 5 – Supersonic Mixed Flows Turbofan Engine Architectures [6-8]

3. THEORETICAL CONSIDERATIONS

The purpose of the thermodynamic analysis of the jet engines is to determine the Design and Off-Design Engine Performances, where the accuracy of the predicted performances depends on the mathematical model and the assumptions considered within.

The objectives of the analysis of the mixed flows turbofan MFTF engine are represented by modeling and simulation, so as to obtain the predicted engine performances, for different flight regimes and various operating regimes. In principle, the calculations are carried out distinctly for the core flow, bypass flow, mixing area and integrating the results in the overall performances, [1-5], [9-14].

The mathematical model of the mixed flows turbofan includes the mathematical model of a turbojet engine, since the core flow calculations describe perfectly the turbojet engine calculations, from the stand point of the fluid flow thermo-dynamical processes, [19-21].

In case of the mixed flows turbofan engine, the mathematical model describing its behavior as close to reality as regards the engine operation and analysis from the thermodynamic standpoint, is based on the following assumptions:

1/ fixed geometry engine,

2/ the work fluid is considered perfect gas,

3/ different species are considered for the work fluid:

a/ air as cold stream within engine intake and compressor,

b/ fuel,

c/ mixture of burned gas as hot stream within combustor, turbine and exhaust unit, 4/ Fuel Specific Energy FSE [kJ/kg] = P_{CI} = 43500 [kJ/kg] at design point, from a range of 40000 [kJ/kg] up to 45000 [kJ/kg],

5/ Brayton cycle is described by isentropic, adiabatic thermodynamic evolutions,

6/ losses are included, which generate an increase in entropy within the Brayton cycle,

7/ the properties of the work fluid: ratio of specific heat k, constant pressure specific heat C_p , gas constant R , as listed in Table 1; the relation between R and C_p is (1).

Other parameters (expressed as non-dimensional coefficients) required for calculating the performances of the engine are:

1/ pressure ratio (i.e. compressor pressure ratio): π_c^*

2/ fan pressure ratio: π_v^*

3/ turbine inlet temperature T_3^* or stagnation specific enthalpy at turbine inlet: i_3^*

4/ air intake pressure loss, σ_{da}^*

5/ adiabatic efficiency on compression for compressor η_c^* and fan η_v^*,

6/ combustion chamber pressure loss, σ_{ca}^*

7/ efficiency of the combustion process, ξ_{ca}^*

8/ adiabatic efficiency on turbine expansion, η_t^*

9/ velocity loss within nozzle exit, φ_{ar}

10/ mechanical efficiency η_m (i.e. shaft transmission efficiency),

11/ bypass ratio: K.

For further developments, the mathematical model of the engine can be expanded with the hypothesis of variable geometry, e.g. in case of engine exit nozzle.

Table 1. Properties of the work fluids

Fluid Type	$k = \frac{C_p}{C_v}$	$C_p\ [\frac{kJ}{kgK}]$	$R\ \left[\frac{J}{kgK}\right]$
Air	1.4	1.005	287.3
Burned Gas	1.33	1.165	288.4

$$C_p = R \cdot \frac{k}{k-1} \tag{1}$$

The thermodynamic analysis of the jet engines and mixed flows turbofan engine as well, supposes the calculation of the performances (thrust F [N], specific thrust F_{sp} [Ns/kg] and specific fuel consumption C_{sp} [kg/Nh], TSFC, for the flight envelope of the aircraft and global range of engine speed regimes $\bar{n}$; such process is also referred as design and off-design performance prediction, [9-14].

$$\bar{n} = \frac{n}{n_{Design}} \tag{2}$$

The mathematical model allows the design and off-design performance prediction of the mixed flows turbofan engine MFTFE, for all the flight regimes that are included within flight envelope and for all the engine operating regimes $\bar{n}$.

The most representative engine operating regimes are:

- Design: $\bar{n}$ =100 %,
- Cruising: $\bar{n} = 90\%$,

- Cruising lowered: $\bar{n} = 85\%$,
- Idle ground: $\bar{n} = 40\%$ and
- Max starting: $\bar{n} = 105\%$.

The results of the performance prediction computations can be summarized in the engine maps, as follows: Altitude Map, Velocity Map and Speed Map. The analysis of the engine maps supposes the consideration of the influence of altitude, flight velocity and engine speed $\bar{n}$ on mechanical work on compression l_c^* (compressor) and l_v^* (fan), pressure ratio π_c^* (compressor) and π_v^* (fan), overall airflow ratio $\dot{M}_{am}$, core flow airflow ratio $\dot{M}_{a1}$, bypass airflow ratio $\dot{M}_{a2}$ and bypass ratio K.

The specificity of the mixed flows turbofan consists in the mixing of the two streams (Core Flow and Bypass Flow, as detailed in Figure 1), resulting the mixture of burned gas from Core Flow and the compressed air from Bypass Flow.

The thermodynamic parameters and the specific thrust are distinctly calculated for Core Flow and Bypass Flow. In addition, for the mixed flows turbofan engine it is required the determination of the fluid parameters (static and stagnation pressure, static and stagnation temperature, velocity) inside the mixing chamber, [15-18] and the combustor fuel – air mixture ratio. The parameters at fan exit and turbine exit are important for calculating the overall engine thrust; the parameters in question are: turbine exit stagnation pressure and stagnation temperature, fan air exit stagnation pressure and stagnation temperature, [1-5], [9-13].

Computation of performances on mixed flows turbofan engine Core Flow

The core flow performances are expressed by the specific thrust F_{sp1} (3), core thrust F_1 (4) and specific fuel consumption C_{sp1} (5).

$$F_{sp1} = m_g \cdot c_{5am} - V, \left[\frac{Ns}{kg}\right] \tag{3}$$

$$F_1 = F_{sp} \cdot \dot{M}_{a1}, [N] \tag{4}$$

$$C_{sp1} = \frac{3600 \cdot m_c}{F_{sp}}, \left[\frac{kg}{Nh}\right] \tag{5}$$

The velocity of the expelled gas c_{5am} (6) comes out after computing the thermodynamic parameters in the mixing area.

$$c_{5am} = \varphi_{ar} \cdot \sqrt{2 \cdot \left\{ \left[i_3^* \cdot \left(1 - \pi_d^* \cdot \sigma_{da}^* \cdot \pi_c^* \cdot \sigma_{ca}^*\right)^{-\left(\frac{kg-1}{kg}\right)} \right] - i_1^* \cdot \left[\frac{(\pi_c^*)^{\frac{k-1}{k}} - 1}{\eta_c^* \cdot \eta_t^* \cdot \eta_m} \right] \right\}} \tag{6}$$

Based on the fuel flow ratio $\dot{M}_c$ and core airflow ratio $\dot{M}_{a1}$ result the flow coefficients: a/ fuel flow coefficient m_c (7) and b/ gas flow coefficient m_g (8):

$$m_c = \frac{\dot{M}_c}{\dot{M}_{a1}} \tag{7}$$

$$m_g = \frac{\dot{M}_g}{\dot{M}_{a1}} \tag{8}$$

Computation of performances on mixed flows turbofan engine Bypass Flow

The bypass flow performances are expressed by the specific thrust F_{sp2} (9) and bypass thrust F_2 (10).

$$F_{sp2} = c_{5am} - V, \left[\frac{Ns}{kg}\right] \tag{9}$$

$$F_2 = F_{sp2} \cdot \dot{M}_{a2}, [N] \tag{10}$$

Computation of overall performances for mixed flows turbofan engine

The overall performances are given by overall specific thrust F_{sp} (11), overall specific fuel consumption C_{sp} (12), overall thrust F (13) and overall air flow $\dot{M}_{am}$ (14):

$$F_{sp} = (1+K)(c_{5am} - V), \left[\frac{Ns}{kg}\right] \tag{11}$$

$$C_{sp} = 3600 \frac{m_c}{(1+K)(c_{5am} - V)}, \left[\frac{kg}{Nh}\right] \tag{12}$$

$$F = F_1 + F_2 = \dot{M}_{am}(1+K)(c_{5am} - V), [N] \tag{13}$$

$$\dot{M}_{am} = \dot{M}_{a1} + \dot{M}_{a2} = (1+K)\dot{M}_{a1}, \left[\frac{kg}{s}\right] \tag{14}$$

Assessing the influence of the engine speed $\bar{n}$ on mechanical work on compression l_c^* (compressor) and l_v^* (fan)

The equation expressing the work balance in case of the mixed flows turbofan engine is (15). The variation of mechanical work of the compressor l_c^* (16) and fan l_v^* (17) with the engine rotor speed $\bar{n}$ (2) is quadratic.

$$l_T^* = l_C^* + K \cdot l_V^* \tag{15}$$

$$l_c^* = l_{c_0}^* \cdot \bar{n}^2 \tag{16}$$

$$l_v^* = l_{v_0}^* \cdot \bar{n}^2 \tag{17}$$

Assessing the influence of the aircraft flight regimes (altitude, Velocity or Mach number) and the engine's operating speed regimes $\bar{n}$

The influence of the aircraft flight regimes (altitude, Velocity or Mach number) and the engine's operating regimes (i.e. engine speed regimes) is expressed by variation of the dynamic pressure ratio π_d^* (18), compressor pressure ratio π_c^* (19), fan pressure ratio π_v^* (20), core airflow ratio $\dot{M}_{a1}$ (21), bypass airflow ratio $\dot{M}_{a2}$ (22) and bypass ratio K (23).

$$\pi_d^* = \frac{p_H^*}{p_H} = \left(\frac{T_H^*}{T_H}\right)^{\left(\frac{k-1}{k}\right)} = \left(1 + \frac{(k-1)}{2} \cdot Mach^2\right)^{\left(\frac{k-1}{k}\right)} = \left(\Theta(Mach)\right)^{\left(\frac{k-1}{k}\right)} \tag{18}$$

$$\pi_c^* = \left[1 + \left(\left(\pi_{c_0}^*\right)^{\frac{k-1}{k}} - 1\right) \cdot \frac{i_0}{i_H^*} \cdot \bar{n}^2 \cdot \frac{\eta_c^*}{\eta_{c_0}^*}\right]^{\left(\frac{k}{k-1}\right)} \tag{19}$$

$$\pi_v^* = \left[1 + \left(\left(\pi_{v_0}^*\right)^{\frac{k-1}{k}} - 1\right) \cdot \frac{i_0}{i_H^*} \cdot \bar{n}^2 \cdot \frac{\eta_v^*}{\eta_{v_0}^*}\right]^{\left(\frac{k}{k-1}\right)} \tag{20}$$

$$\dot{M}_{a1} = \dot{M}_{a1_0} \cdot \frac{\pi_c^*}{\pi_{c_0}^*} \cdot \pi_d^* \cdot \frac{p_H}{p_0} \tag{21}$$

$$\dot{M}_{a2} = \dot{M}_{a20} \cdot \frac{\pi_v^*}{\pi_{v_0}^*} \cdot \pi_d^* \cdot \frac{p_H}{p_0} \tag{22}$$

$$K = K_0 \left(\frac{\pi_v^*}{\pi_{v_0}^*}\right)\left(\frac{\pi_{c0}^*}{\pi_c^*}\right) q(\bar{\lambda}_{52}) \sqrt{\frac{(i_0 + l_{v_0}^*)}{(i_1^* + l_{v_0}^*)}} \tag{23}$$

The mixing area – specificity feature of the mixed flows turbofan engine

Prior to calculate the velocity of the expelled gas c_{5am} (6), the thermodynamic parameters of flow (e.g. field distributions of velocity, static pressure, static temperature, static enthalpy and entropy, stagnation pressure, stagnation temperature, stagnation enthalpy and entropy, gas fluid flow rate) in the mixing area must be completely determined.

Based on the thermodynamic flow function $q(\lambda)$ (24), expressed with the Chaplygin's number λ (25) as variable, a new non-dimensional function $q(\bar{\lambda}_{52})$ (26) can be introduced, where its variable $\bar{\lambda}_{52}$ is the ratio of the values of the flow functions appraised in the mixing section, for the current operating regime $q(\lambda_{52})$ versus the design regime $q(\lambda_{52\_0})$.

Unlike the definition of Mach number (27), the Chaplygin's number is introduced as in relation (26).

$$q(\lambda) = \lambda\left[\frac{k+1}{2}\left(1-\left(\frac{k-1}{k+1}\right)\lambda^2\right)\right]^{\frac{1}{k-1}} \quad (24)$$

$$q(\bar{\lambda}_{52}) = \frac{q(\lambda_{52})}{q(\lambda_{52\_0})} \quad (25)$$

$$\lambda = \frac{object\_speed}{local\_critical\_speed} \quad (26)$$

$$Mach = \frac{object\_speed}{speed\_of\_sound} \quad (27)$$

Description of computational algorithm

Design and Off-Design Performance Prediction (also referred as Performance Analysis) in case of Mixed Flows Turbofan Engine supposes the completion of three phases, [1-5]:

 # Phase 1/ - the determination of the overall engine's performances: overall specific thrust F_{sp} (11), overall specific fuel consumption C_{sp} (12), overall thrust F (13) and Brayton cycle, for the design speed regime $\bar{n}$, at SLS, ISA conditions (28), i.e. static pressure, static temperature and static specific enthalpy, for flight velocity or Mach number = 0, [9-13].

$$p_0 = 1.01325\ [bar] \qquad T_0 = 288\ [K] \qquad i_0 = C_p \cdot T_0\ \ [kJ/kg] \quad (28)$$

 # Phase 2/ - the determination of the overall engine's performances: overall specific thrust F_{sp} (11), overall specific fuel consumption C_{sp} (12), overall thrust F (13) at different flight regimes (i.e. altitude H ranging from 0 up to 12 [km] and flight Mach number) and engine rotor speed $\bar{n}$, which usually are expressed by Altitude Map, Velocity Map, Speed Map which define the Engine's Operating Maps, [9-14], [19-21], [22-24].

 # Phase 3/ - is dedicated to refining the investigation, by focusing on the influence of the exit unit parameters such as the exit nozzle velocity loss coefficient φ_{ar} and compressor efficiency η_c^*, as well as the influence of the flight regimes and engine operating speed regimes $\bar{n}$ on the overall thrust overall thrust F (13), as the main performance of the mixed flows turbofan MFTF engine.

The mathematical model is of versatile use, since the numerical simulations can be done in a similar way, but in purpose to highlight the influence of other thermodynamic parameters (such as turbine inlet temperature, efficiency on compression within fan, Low Pressure Compressor LPC and High Pressure Compressor HPC) on the overall thrust.

4. NUMERICAL SIMULATIONS AND RESULTS

The study case is a mixed flows turbofan, as indicated in Fig. 3, defined by the main design parameters of the mixed flows turbofan engine, listed in Table 2: overall pressure ratio π_c^*, bypass ratio K, overall airflow rate $\dot{M}_a$ [kg/s] are given in jet engine catalogue, while the core airflow rate $\dot{M}_{a1}$ [kg/s], bypass airflow rate $\dot{M}_{a2}$ [kg/s] and the fan pressure ratio π_v^* results from calculations based on the engine's design data.

Table 2. Main parameters of the mixed flows turbofan engine

Parameter		Units
Overall Pressure Ratio	$\pi_c^* = 22$	[---]
Bypass Ratio	$K = 2.9$	[---]
Overall Airflow Rate	$\dot{M}_a = 65.772$	[kg/s]
Core Airflow Rate	$\dot{M}_{a1} = 37.18$	[kg/s]
Bypass Airflow Rate	$\dot{M}_{a2} = 107.82$	[kg/s]
Fan Pressure Ratio	$\pi_v^* = 1.77$	[---]

Based on the computational algorithm described above, the authors have developed an in-house code purposed to determine the variation of the mixed flows turbofan engine overall performances: overall specific thrust F_{sp} (11) [Ns/kg], overall specific fuel consumption C_{sp} (12) [kg/Nh], overall thrust F (13) [N], with flight Mach number, flight altitude and engine operational regimes $\bar{n}$: Design, Cruising and Ground Idling, presented in Table 3.

Table 3. Flight regimes and engine operational regimes

Flight regimes		Units
Altitude	$H \in \{0, 2, 4, 6, 8, 10\}$	$[km]$
Mach number	Mach $\in \{0; 0{,}2; 0{,}4; 0{,}6; 0{,}8; 1{,}0\}$	[---]
Engine operational regimes $\bar{n}$		[% *engine-design-speed*]
Design	$\bar{n} =$100 %	[% *engine-design-speed*]
Cruising	$\bar{n} =$ 90%	[% *engine-design-speed*]
Ground Idling	$\bar{n} =$ 40%	[% *engine-design-speed*]

The current analysis is focused on highlighting the influence of the exit nozzle velocity loss coefficient φ_{ar} and compressor efficiency η_c^* (see the values listed in Table 4), as the most significant parameters of the mixed flows turbofan engine, on the overall thrust.

Table 4. Investigation Variable parameters

Parameter		Units
Compressor efficiency	$\eta_c^* = 0.82; 0.84; 0.86$	[---]
Exit Nozzle Velocity Loss Coefficient	$\varphi_{ar} = 0.85; 0.90; 0.95$	[---]

In case of the mixed flows turbofan engine, due to its military applicability, the overall thrust is the most important engine performance and therefore it is monitored and controlled with priority.

The results from the simulation the Mixed Flows Turbofan Engine are summarized and presented graphically, in Fig. 6 – Fig. 8.

In Fig. 6 – Fig. 8 there are presented the variation of overall thrust $F[N]$ for flight Mach number ranging from 0 up to 1 and the flight altitude $H \in \{0, 2, 4, 6, 8, 10\}\ [km]$.

In Fig. 6 there is expressed the variation of overall thrust $F[N]$ in case of the 100% Design Regime, compressor efficiency $\eta_c^* = 0.84$ and exit nozzle velocity loss coefficient ranging $\varphi_{ar} = 0.85; 0.90; 0.95$.

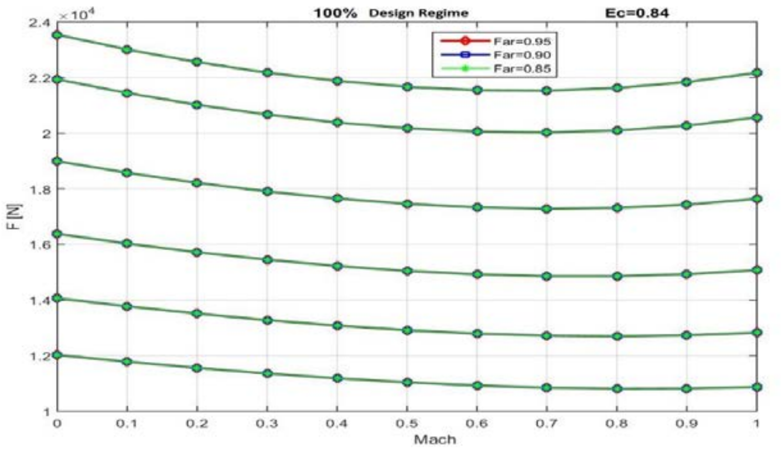

FIG. 6 – Variation of Thrust [N] versus Mach number; Engine Regime = Design

In Fig. 7 there is expressed the variation of overall thrust $F[N]$ in case of the 90% Cruise Regime, compressor efficiency $\eta_c^* = 0.84$ and exit nozzle velocity loss coefficient ranging $\varphi_{ar} = 0.85; 0.90; 0.95$.

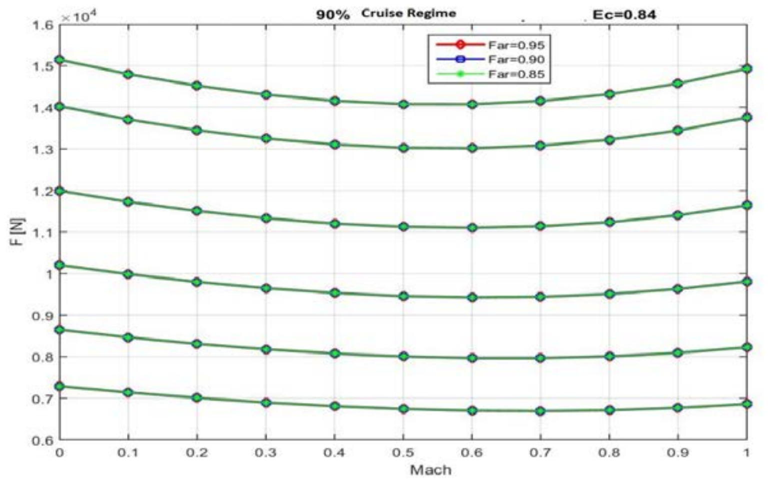

FIG. 7 – Variation of Thrust [N] versus Mach number; Engine Regime = Cruise

Figure 8 expresses the variation of overall thrust $F[N]$ in case of the 40% Ground Idling Regime, compressor efficiency $\eta_c^* = 0.84$ and exit nozzle velocity loss coefficient ranging $\varphi_{ar} = 0.85; 0.90; 0.95$.

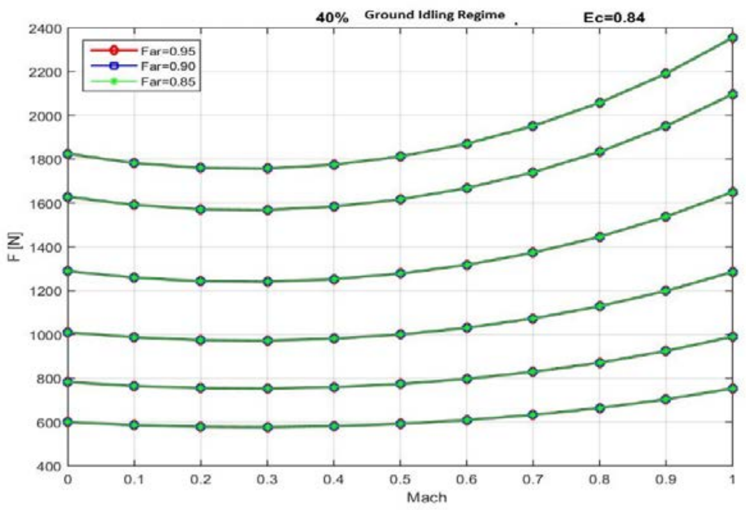

FIG.8 – Variation of Thrust [N] versus Mach number; Engine Regime = Ground Idling

5. FINAL CONCLUSIONS

The investigation presented in this paper is focused on the variation of the overall thrust $F[N]$ of the mixed flows turbojet engine due to the variations ranging for flight Mach number $\in \{0; 0{,}2; 0{,}4; 0{,}6; 0{,}8; 1{,}0\}$, flight altitude $H \in \{0, 2, 4, 6, 8, 10\}$ $[km]$ and engine operational regimes $\bar{n}$: Design 100 %, Cruising = 90%, and Ground Idling = 40%.

The objective of this study is to highlight the variation of engine's thrust for given perturbations of the compressor efficiency $\eta_c^* = 0.84$ and exit nozzle velocity loss coefficient ranging $\varphi_{ar} = 0.85; 0.90; 0.95$.

The results of the numerical simulations for performance prediction of the mixed flows turbofan engine, focused on the overall thrust, are concluded in Fig. 6 ÷ Fig. 8.

The graphical results can be interpreted such that the effect of small perturbations in the exit nozzle velocity loss coefficient ranging φ_{ar} do not affect the overall thrust, in case of constant compressor efficiency η_c^*.

For the flight altitude 10 [km], from Fig.6 there results that the overall thrust is minimum for the Mach number = 0.7, at Design regime 100%, while from Fig. 7 there results the overall thrust as minimum for the Mach number = 0.6, at Cruise regime 90%, in comparison with Fig. 9 that indicates the overall thrust as minimum for the Mach number = 0.3, at Ground Idling regime 40%. As a matter of fact, the Ground Idling regime takes place for SLS, ISA conditions, indicating the flight altitude 10 [km], so therefore, from Fig. 9, one can consider that the overall thrust is minimum for the Mach number $\in [0{,}2 - 0{,}3]$.

The potential future developments of this study can be guided to the complete determination of the Engine Maps (1/ Altitude Map. 2/ Velocity Map, 3/ Speed Map), Engine Universal Map, which can be represented in non-dimensional coordinates.

The importance of this study consists of providing reliable input data for further expansions of the study towards the mixed flows turbofan engine automat control and the design and optimization of mixed flows turbofan engine automatic control system.

REFERENCES

[1] N. Cumpsty, *Jet Propulsion, A Simple Guide to the Aerodynamic and Thermodynamic Design and Performace of the Jet Engines*, Cambridge University Press, 2003, 2009, ISBN 978-0-521-54144-2;
[2] Thaddeus D. Fowler (Editor), *Jet Engines and Propulsion Systems for Engineers*, Human Resource Development, General Electric Aircraft Engines, 1989;
[3] J. D. Mattingly, *Elements of Propulsion and Gas Turbine and Rockets*, American Institute of Aeronautics and Astronautics Education Series, Inc. Reston, VA,.2006;
[4] J. D. Mattingly, *Elements of Gas Turbine Propulsion*, Mc Graw-Hill, 1996;
[5] S. Farokhi, *Aircraft propulsion*, second edition, Wiley and sons, 2014;
[6] ***, Rolls Royce, *The Jet Engine*, fifth edition, ISBN 0 902121 2 35, The Technical Publications Department Rolls-Royce plc, Derby, England;
[7] ***, Powerplant, JAA ATPL Training, JEPPESEN, Atlantic Flight Training Ltd;
[8] https://www.google.com/search/low+bypass+turbofan+engine/ images;
[9] Wilfried Wisser, *Generic Analysis Methods for Gas Turbine Engine Performance, The development of the gas turbine simulation program GSP*, PhD Thesis, NLR and TU Delft, 2015;
[10] ***, *Compressor and Turbine Maps for Gas Turbine Performance Computer Programs*, Issue 3, GasTurb GmbH, 2013;
[11] ***, *GasTurb 12, Design and Off-Design Performance of Gas Turbines,* GasTurb GmbH, 2015;
[12] S. M. Eastbourn, *Modeling and simulation study of a dynamic turbofan engine using Matlab Simulink*, M. Sc. A.E. Dissertation, Wright State University, 2012;
[13] S. Zak, *Turbojet Engine Modeling*, School of Electrical and Computer Engineering, Purdue University, 2014;
[14] Hans de Ryck, *Turbofan design for the commercial aircraft*, PhD Thesis, Warsaw University of Technology, Faculty of Power and Aeronautical Engineering, Warsaw, Poland, Katholiecke Hogeschool Brugge-Oostende, Department Industriële Wetenschappen & Technologie, Oostende, België, 2008;
[15] C. Rotaru, M. Mihaila-Andres, G.M. Pericle, R. I . Edu, *Thermodynamic performances of the turbojet combustion chambers – numerical evaluation*, Proceedings of the 2014 International Conference on Mechanics, Fluid Mechanics, Heat and Mass Transfer, p. 86-91, 2014;
[16] V. Prisacariu, I. Cîrciu, *Considerations Regarding the Performances of the Combustion Chambers for Turbojet Engines*, Review of the Air Force Academy, No 2 (32) 2016, DOI: 10.19062/1842-9238.2016.14.2.7;
[17] C. Rotaru, M. Andres-Mihaila, G.M. Pericle, *An Extended Combustion Model for the Aircraft Turbojet Engine*, International Journal of Turbo & Jet-Engines, 3/2014, p.229-237, 2014;
[18] C. Rotaru, I. Cîrciu, C. Arama, C. Constantinescu, *Aspects regarding velocity distribution in the secondary zone of a gas turbine combustor*, Review of the Air Force Academy, 2/2015, DOI: 10.19062/1842-9238.2015.13.3.5, p. 33-38, 2015;
[19] F. Zare, Dr. Arpad Veress, K. Beneda, *Simplified mathematical model for a single spool and no by-pass jet engine*, RTK Conference, BME, 2013;
[20] H. Asgari, X. Chen, R. Sainudin, *Modeling and simulation of gas turbines*, Intl. Journal Modelling, Simulation and Control, 2013;
[21] S. C. Uysal, *High by-pass ratio turbofan engines aero-thermodynamic design and optimization*, PhD Thesis, The Graduate School of Natural and Applied Sciences, Middle East Technical University, 2014;
[22] NASA Technical Memorandum TM X-3014, *A generalized hybrid computer program for studying turbojet or turbofan engine dynamics*, John Szuch, Cleveland, Ohio, 1974;
[23] NASA Technical Memorandum 83446 (NASA - TM 83446), *Digital Computer Program for Generating Dynamic Turbofan Engine Models (DIGTEM)*, C.J. Daniele, S. M. Krosel, J. R. Szuch, E. J. Westerkamp, Lewis Research Center, Cleveland, Ohio, 1983;
[24] NASA Technical Memorandum TM X-71726 (NASA - TM X-71726), *An Application of Modern Control Theory to Jet Propulsion Systems*, Walter C. Merrill, Lewis Research Center, Cleveland, Ohio, 1975.